Ethane / Nitrous Oxide Mixtures as a Green Propellant to Substitute Hydrazine: Validation of Reaction Mechanism

C. Naumann*, C. Janzer, U. Riedel

German Aerospace Center (DLR), Institute of Combustion Technology
Pfaffenwaldring 38-40, 70569 Stuttgart, Germany

Abstract
The combustion properties of propellants like ethane / nitrous oxide mixtures that have the potential to substitute hydrazine or hydrazine / dinitrogen tetroxide in chemical propulsion systems are investigated. In support of CFD-simulations of new rocket engines powered by green propellants ignition delay times of ethane / nitrous oxide mixtures diluted with nitrogen have been measured behind reflected shock waves at atmospheric and elevated pressures, at stoichiometric and fuel-rich conditions aimed for the validation of reaction mechanism. In addition, ignition delay time measurements of ethene / nitrous oxide mixtures and ethane / O_2 / N_2 - mixtures with an O_2:N_2 ratio of 1:2 as oxidant at the same level of dilution are shown for comparison. Finally, the ignition delay time predictions of a recently published reaction mechanism by Glarborg et al. are compared with the experimental results.

Introduction

Hydrazine and hydrazine derivatives like monomethyl hydrazine (MMH) and unsymmetrical dimethyl hydrazine (UDMH) are used for spacecraft propulsion applications in various technological contexts despite their drawback of being highly toxic. Today, hydrazine consumption for European space activities is on the order of 2-5 tons per year. However, if the impact of the REACH (Registration, Evaluation, Authorisation and Restriction of Chemicals) regulation should come into full force in the upcoming years, hydrazine use in Europe will be severely restricted, although the propellant may remain available from other sources outside Europe. Nevertheless, green propellants for European space activities are an accepted challenge for research and for technology development. Similar to research programmes in the U.S. initiated by DARPA (see [1], [2]), DLR investigates the combustion properties of propellants like ethene or ethane / nitrous oxide mixtures that have the potential to substitute hydrazine or hydranzine / dinitrogen tetroxide in chemical propulsion systems (see [3], [4], [5]). Furthermore, cryogenic mixtures of ethene or ethane with nitrous oxide are intended to be used as monopropellants, thus reducing the weight of the orbiter's propulsion systems. Data from model combustors operated at DLR's rocket propulsion test site at Lampoldshausen (Germany) in combination with investigations of fundamental combustion properties provide valuable test cases to be analysed by CFD computations, thus gaining better insights to the specific design requirements of new rocket engines powered by green propellants.

For these reasons, this contribution deals with the measurement of ignition delay times of ethane / nitrous oxide mixtures for the purpose of validating appropriate reaction mechanism to support CFD combustor simulations. Ignition delay times of stoichiometric and fuel-rich mixtures of C_2H_6 / N_2O diluted 1:5 with nitrogen have been investigated behind reflected shock waves at initial pressures of $p_{nominal}$ = 1, 4, and 16 bar. The results are compared to ignition delay time measurements of stoichiometric C_2H_4 / N_2O mixtures (see [6], [7], [8]). Complementary, ignition delay times of the corresponding oxygen based reactive mixture C_2H_6 / (1/3 O_2 + 2/3 N_2) have been measured, too. Thereafter, the predictions of a recently published reaction mechanism by Glarborg et al. [9] containing the required H/O/C/N-chemistry are compared with the ignition delay time measurements. Finally, sensitivity analyses of the reaction systems investigated round off this contribution.

Experiment

The experiments were carried out at DLR's shock tube facility at Stuttgart. The shock tube used (see Figure 1) has an internal diameter of 98.2 mm. It is divided by aluminium diaphragms into a driver section of 5.18 m and a driven section of 11.12 m in length. Driver and driven section are separated by a small intermediate volume establishing a double-diaphragm operation. The driver section was loaded with mixtures of helium and argon controlled by Bronkhorst mass flow controllers to achieve tailored interface conditions.

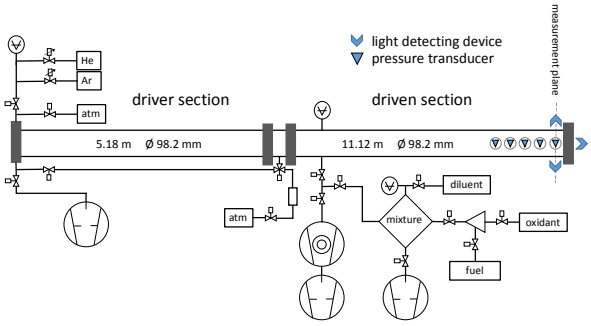

Figure 1: Sketch of DLR's ∅ 98.2 mm shock tube. The measurement plane is located 10 mm in front of the end plate.

* Corresponding author: clemens.naumann@dlr.de

The driven section was pumped down to pressures below 10^{-6} mbar by a turbomolecular pump. The ignitable mixtures of C_2H_6 / N_2O, C_2H_4 / N_2O and C_2H_6 / (1/3 O_2 + 2/3 N_2) diluted with nitrogen were prepared manometrically in stainless steel storage cylinders, which were evacuated using a separate turbomolecular pump. Gases used were delivered by LINDE AG (purities: N_2O: 99.999 %, C_2H_6: 99.95 %, C_2H_4: 99.95 %, O_2: 99.9999 %, N_2: 99.9999 %). A dilution of 1:5 with nitrogen was applied to all mixtures. Due to the very short deflagration-to-detonation time of the mixtures containing nitrous oxide as oxidant, the dilution reduces the dynamic load to the shock tube during ignition and deflagration especially after compressing the reactive mixtures to an initial pressure of p = 16 bar behind reflected shock waves. The arrival of the incident and reflected shock waves or the deflagration wave was measured along the shock tube using five piezoelectric pressure gauges (PCB 113B24). The temperature and pressure directly behind the reflected shock wave were computed from the incident shock speed – derived from the x-t diagram – using a one-dimensional shock model.

Ignition was observed by two detection methods: First, by measuring pressure profiles with piezoelectric gauges (PCB 113B24 and Kistler 603B) located at a distance of 10 mm to the end plate. Both pressure gauges were completely shielded by at least 1 mm RTV106 high temperature silicone rubber to reduce heat transfer and thus signal drift. Second, the CH(A) emission at 431 nm was selected by narrow band pass filters (Hugo Anders, FWHM = 5 nm), detected with photomultipliers (HAMAMATSU R3896) and amplified by logarithmic amplifiers (FEMTO HLVA-100) at the measurement plane located 10 mm away from the end plate ('radial') and through the end plate window ('axial'). All ignition delay time values shown in this paper were determined by measuring the time difference between the initiation of the system by the reflected shock wave at the end plate and the occurrence of the first CH(A) maximum at the side port and alternatively through the end plate window. Moreover, the radial ignition delay times were blast-wave corrected using the deflagration velocity derived from the ignition delay time measurements at the highest temperatures of each series.

Without tailoring, i.e. adapting the impedance of the driver gas to that of the test gas behind the incident shock wave close to the contact 'surface', the maximum observation period for this shock tube is limited to less than 3 ms because of the decompression wave generated by the accelerated reflected shock front after passing through the contact surface. Adjusting the impedance of the driver gas by adding argon to the helium can avoid this decompression wave, thus extending the observation time until the reflected rarefraction fan originated at the burst diaphragm decompresses the shock heated mixture after about 8 ms. In either case, there is a post-shock compression that cannot be avoided without taking additional measures like dynamic mass flow reduction of the driver gas [11]. This post-shock pressure rise is a consequence of the attenuation of the reflected shock caused by the interaction with the growing boundary layer formed behind the incident shock. Due to the incident test gas / reflected shock front velocity mismatch, there will be a residual velocity of the shock heated and compressed gas behind the reflected shock front towards the end plate. This residual velocity and thus the post-shock pressure rise will become the stronger the more the reflected shock front will be attenuated. For the non-tailored case, this pressure rise can mostly be attributed by a dp/dt = const. approach. Its magnitude depends mainly on the inlet pressure, the Mach number, the bath gas and the shock tube's length and diameter, all affecting the boundary layer growth, the timing and the shock wave / boundary layer interaction. In the tailored case, the pressure rise will also start at a constant rate but due to the missing acceleration of the reflected shock front at the contact surface, the pressure will increase further non-linearly until a maximum has been reached (see pressure profile in Figure 2). From here on, if tailoring has been done right, the pressure profile remains more or less at a constant level because of a weak attenuation of the reflected shock front in the driver gas, until the reflected rarefraction fan decompresses the mixture or the mixture ignites, whatever happens first.

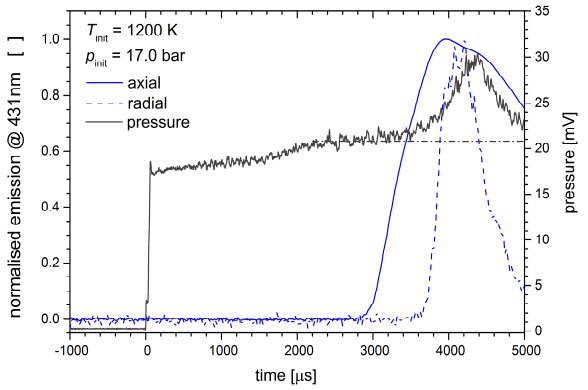

Figure 2: Ignition delay time measurement of a C_2H_6 / N_2O / N_2 - mixture with extended observation period; the post-shock pressure rise ceases after 2.1 ms at p / p_{init} ≈ 1.25 (dashed line) followed by pressure rise due to heat release.

To take this post-shock compression into account when calculating ignition delay time with a reaction model, this characteristic and facility dependent pressure rise has to be provided to the energy equation as $p = p(t)$ assuming adiabatic isentropic conditions for the period of observation. In order to attain an answer from the reaction model even if the maximum experimental observation period is over, the pressure profile can be extrapolated appropriately, i.e. linearly as indicated by the dashed horizontal line in Figure 2.

Ignition Delay Time Measurements

Firstly, the ignition delay times of a stoichiometric C_2H_6 / N_2O mixture diluted 1:5 with nitrogen are compared to the same mixture constituents, but at an equivalence ratio of $\Phi = 2$, at initial pressures of 1, 4 and 16 bar. As shown in Figure 3 the stoichiometric mixture at initial pressures of 4 and 16 bar ignites faster than the fuel-rich mixture within the range of temperatures tested. In contrast to this, the ignition delay times of both mixtures at an initial pressure of 1 bar tend to overlap in the high temperature regime. Moreover, approaching lower temperatures the apparent activation energy of the reactive system sharply increases for $\Phi = 2$ at about 1600 K and for the stoichiometric mixture at about 1450 K.

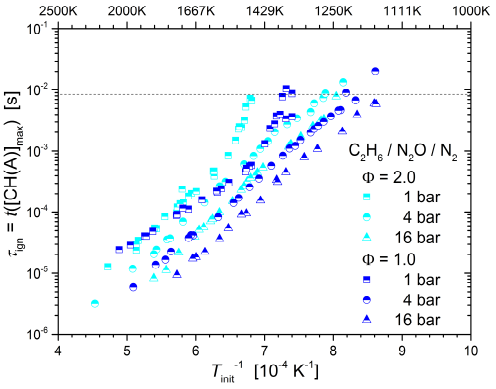

Figure 3: Ignition delay times of ethane / nitrous oxide mixtures diluted 1:5 with nitrogen at stoichiometric and fuel-rich equivalence ratios at initial pressures of 1, 4 and 16 bar. Only axially measured emission data are shown.

Secondly, the measured ignition delay times of a stoichiometric C_2H_6 / N_2O mixture diluted 1:5 with nitrogen are compared to an equivalent C_2H_4 / N_2O mixture as shown in Figure 4.

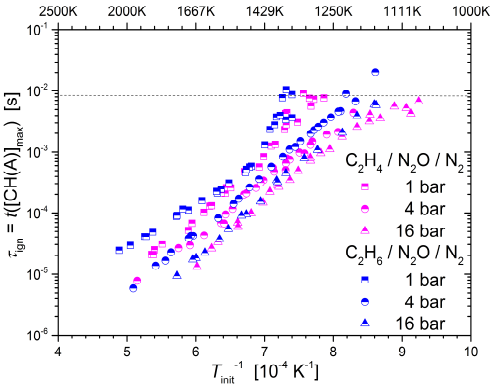

Figure 4: Ignition delay times of stoichiometric ethane / nitrous oxide and ethene / nitrous oxide mixtures diluted 1:5 with nitrogen at initial pressures of 1, 4 and 16 bar. Only axially measured emission data are shown.

In contrast to the distinct difference between the ignition delay times of ethane at different equivalence ratios and at elevated pressures as seen in Figure 3 above, a difference between ethane and ethene at stoichiometric mixture conditions is only noticeable in the lower temperature regime at initial pressures of 4 and 16 bar as seen in Figure 4. Here it should be noted, that according to the post-shock pressure rise at longer observation periods, i.e. at lower initial temperatures, the ignition delay times tend to become shorter due to the increasing temperature induced by the pressure increase, especially at elevated initial pressures. On the other hand, an clear distinction can be made between the ignition delay times of ethane and ethene at an initial pressure of 1 bar.

Thirdly, the measured ignition delay times of a stoichiometric C_2H_6 / N_2O mixture diluted 1:5 with nitrogen are compared to those of a corresponding C_2H_6 / (1/3 O_2 + 2/3 N_2) mixture again at initial pressures of 1, 4 and 16 bar as shown in Figure 5 below.

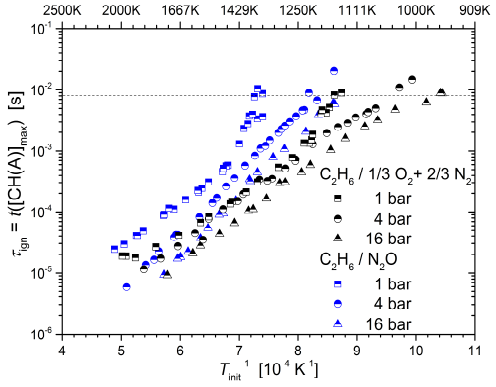

Figure 5: Ignition delay times of stoichiometric ethane / nitrous oxide and ethane / (1/3 O_2 + 2/3 N_2) mixtures diluted 1:5 with nitrogen at initial pressures of 1, 4 and 16 bar. Only axially measured emission data are shown.

Obviously, the C_2H_6 / (1/3 O_2 + 2/3 N_2) mixture ignites faster or at least at the same time at every initial pressure. At an initial pressure of 1 bar, the already described change of the apparent activation energy is also observed, but at a lower temperature of about 1200 K. Again, for initial pressures of 4 and 16 bar post-shock pressure rise at longer observation periods have to be considered, reducing ignition delay time.

Modelling

The recently published reaction mechanism by Glarborg et al. [9] has been used to compare the experimental results with the ignition delay time predictions. For a better comparison, the reaction mechanism has been extended with respect to the excited species OH(A) and CH(A) as proposed by Kathrotia et al. [10]. Thus, the time of maximum [CH(A)] has been defined as 'ignition delay time', i.e. $\tau_{ign} = t([CH(A)]_{max})$. Next, collision enhancement factors (CEF) for C_2H_4, C_2H_6 and N_2O have been

supplemented for all reactions with collisional partners involved. The collision enhancement factors were estimated to $CEF(C_2H_4) = CEF(C_2H_6) = 3$, if the reaction was scaled to $CEF(N_2) = 1$. If already specified, $CEF(C_2H_4)$ was set equal to $CEF(C_2H_6)$. The $CEF(N_2O)$ was estimated to be equal to $CEF(CO_2)$. Finally, high temperature dissociation reactions for N_2, NO, and CO completed the modification anticipating laminar flame speed measurements and modelling (see [6]).

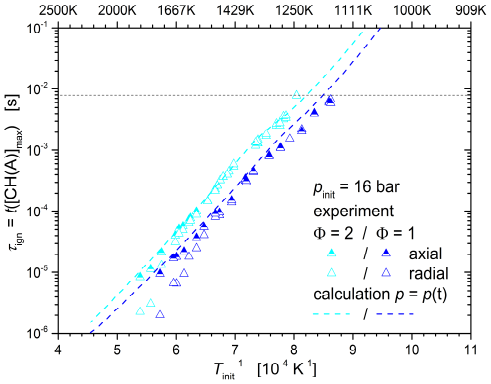

Figure 6: Ignition delay times and model predictions of Glarborg et al. [9] for stoichiometric and fuel-rich ethane / nitrous oxide mixtures diluted 1:5 with nitrogen using experimentally derived pressure profiles for an initial pressure of 16 bar.

Figure 6 illustrates the measured and predicted ignition delay times for the ethane / nitrous oxide mixtures at stoichiometric and fuel-rich conditions for an initial pressure of 16 bar (see Figure 3 for the complete series). Here, the experimental data for the axial measurements of $t([CH(A)]_{max})$ as well as the blast-wave corrected radial measurements are shown.

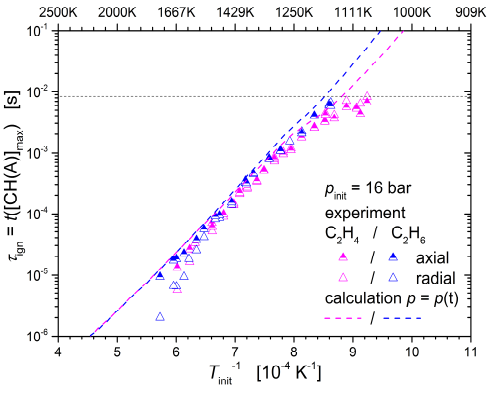

Figure 7: Ignition delay times and model predictions of Glarborg et al. [9] for stoichiometric ethene / nitrous oxide and ethane / nitrous oxide mixtures diluted 1:5 with nitrogen using experimentally derived pressure profiles for an initial pressure of 16 bar.

Obviously, the blast-wave corrected radially measured ignition delay times deviate significantly from the predicted and axially measured ones. The average velocity of the deflagration wave determined from the experiments at the highest temperatures was around 750 m/s, thus assuming a detection delay of about 13.5 µs between end plate and measurement plane for idealised conditions. Nevertheless, the tendency with respect to equivalence ratio as well as the prediction over three orders of magnitude is reproduced well.

Next, Figure 7 represents the measured and predicted ignition delay times for the stoichiometric ethene / nitrous oxide and the ethane / nitrous oxide mixtures also for an initial pressure of 16 bar (see Figure 4 for the complete series). As before, there is a significant difference between axially and radially derived ignition delay times at the highest temperatures. Likewise to the variation of equivalence ratio of the ethane / nitrous oxide mixtures in Figure 6, the tendency with respect to the fuel - ethane or ethene – is also reproduced well using experimentally deduced pressure profiles. It should be remarked that the difference in ignition delay times with respect to the fuel is mainly caused by the higher reactivity of ethene compared to that of ethane at lower temperatures.

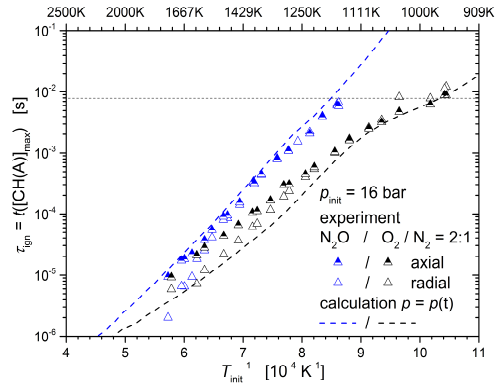

Figure 8: Ignition delay times and model predictions of Glarborg et al. [9] for stoichiometric ethane / nitrous oxide and ethane / (1/3 O_2 + 2/3 N_2) mixtures diluted 1:5 with nitrogen using experimentally derived pressure profiles for an initial pressure of 16 bar.

Finally, ignition delay times and model predictions for the stoichiometric ethane / nitrous oxide and the ethane / (1/3 O_2 + 2/3 N_2) mixtures are presented in Figure **8** for an initial pressure of 16 bar (see Figure 4 for the complete series). In contrast to the ignition delay times of the ethane and ethene / nitrous oxide mixtures at high temperatures, the model predictions for the ethane / (1/3 O_2 + 2/3 N_2) mixture are now closer to the blast wave corrected radially measured ignition delay times. The influence of the post shock pressure rise on the ignition delay times is reproduced fairly well by the reaction model in combination with the experimentally derived pressure profile affecting ignition delay times above 2 ms. For an initial pressure of 1 bar, as illustrated in Figure 9, the predictions reproduce the experiments very well. Again, the change of the apparent activation energy at 1250 K is predicted by trend but at a lower temperature.

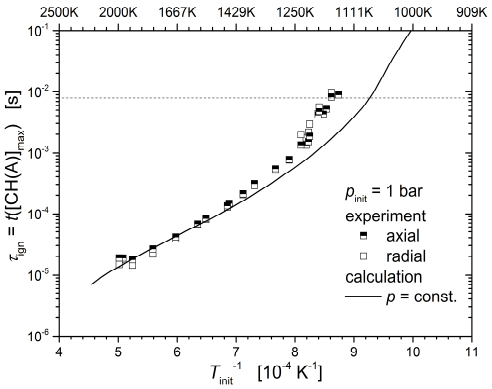

Figure 9: Ignition delay times and model predictions of Glarborg et al. [9] for stoichiometric ethane / nitrous oxide and ethane / (1/3 O_2 + 2/3 N_2) mixtures diluted 1:5 with nitrogen at a initial pressure of 1 bar.

Sensitivity Analysis

In the following section, ignition delay time sensitivity analyses with respect to the rate coefficient of each reaction ($d\tau_{ign} / dk_i$) are presented for the ethane / nitrous oxide mixtures at stoichiometric (Figure 10) and fuel-rich conditions ($\Phi = 2$, Figure 11), as well as for the stoichiometric ethene / nitrous oxide and ethane / (1/3 O_2 + 2/3 N_2) mixtures (Figure 12 and Figure 13). The calculations have been performed at constant pressure of 16 bar. The sensitivity coefficient of the i-th reaction is defined as $S_i = k_i^{ref} / \tau_{ign}^{ref} (d\tau_{ign} / dk_i)$ where the superscript 'ref' means 'at initial conditions'. The sensitivity coefficients S_i at all temperatures are sorted in descending order according to S_i (T = 1400 K).

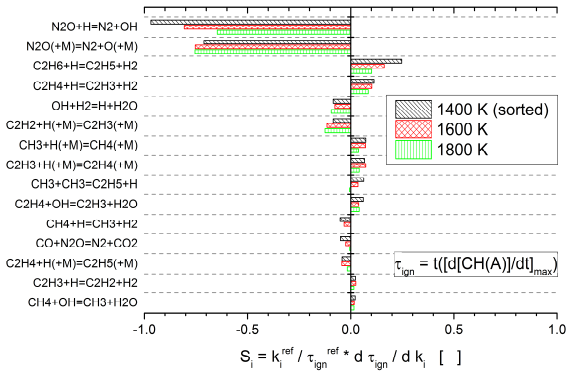

Figure 10: Sensitivity coefficients for the stoichiometric ethane / nitrous oxide mixture diluted 1:5 with nitrogen at a pressure of 16 bar calculated with the reaction mechanism of Glarborg et al. [9].

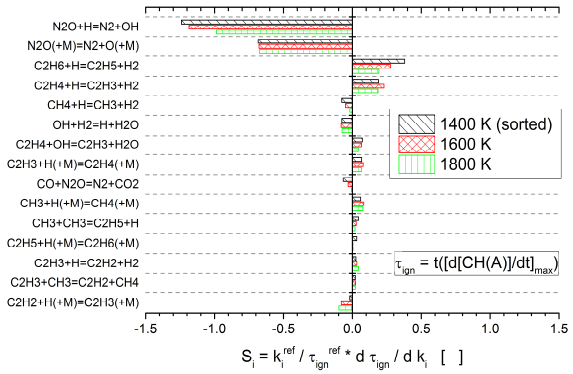

Figure 11: Sensitivity coefficients for the fuel-rich ($\Phi = 2$) ethane / nitrous oxide mixture diluted 1:5 with nitrogen at a pressure of 16 bar calculated with the reaction mechanism of Glarborg et al. [9].

Besides the unimolecular decomposition of nitrous oxide, ignition in the ethane / nitrous oxide reaction system is controlled by the interplay of H-producing reactions with $N_2O+H=N_2+OH$ (see Figure 10 and Figure 11). Hydrogen abstraction and subsequent dissociation of C_2H_5 and C_2H_3 in combination with $OH+H_2=H+H_2O$ provide H-atoms to keep on going.

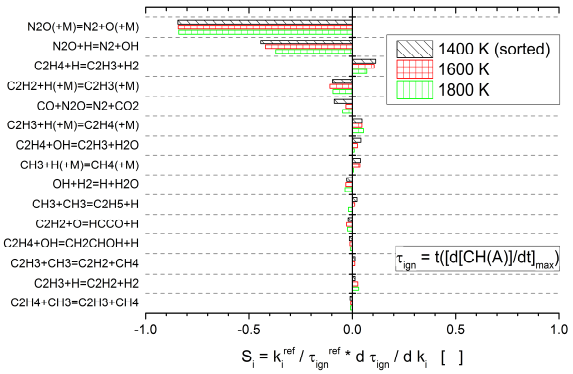

Figure 12: Sensitivity coefficients for the stoichiometric ethene / nitrous oxide mixture diluted 1:5 with nitrogen at a pressure of 16 bar calculated with the reaction mechanism of Glarborg et al. [9].

The sensitivity analysis of the ethene / nitrous oxide reaction system in Figure 12 indicates that the formation of H-atoms turns out to be a bit more difficult than in the ethane / nitrous oxide reaction system, wherefore the sensitivity of the N_2O decomposition reaction exerts a dominating influence.

Interestingly, the reaction $CO+N_2O=N_2+CO_2$ is found among the 15th most sensitive reactions with respect to the ignition delay time of ethane or ethene / nitrous oxide mixtures.

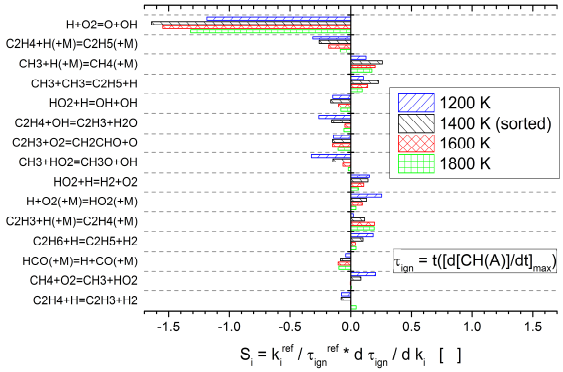

Figure 13: Sensitivity coefficients for the stoichiometric ethane / (1/3 O_2 + 2/3 N_2) mixture diluted 1:5 with nitrogen at a pressure of 16 bar calculated with the reaction mechanism of Glarborg et al. [9].

Finally, the sensitivity analysis of the stoichiometric ethane / (1/3 O_2 + 2/3 N_2) mixture presented in Figure 13 reflects the well established hydrocarbon oxidative scheme.

Conclusions

The reaction mechanism by Glarborg et al. [9] reproduces all ethan / nitrous oxide and ethene / nitrous oxide mixtures at initial pressures of p_{init} = 4 and 16 bar fairly well. At an initial pressure of p_{init} = 1 bar, the predictions tend towards longer ignition delay times compared to the measurements. Only the change in the apparent activation energy at inital pressures of 1 bar (see Figure 3 to Figure 5) is not reproduced. It is still in question, if this is an experimental interference, i.e. induced by driver gas shooting through at very low inlet pressures, or an effect of the reaction kinetics, i.e. the well defined and distinct temperature of the apparent actication energy.

With respect to the ethane / (1/3 O_2 + 2/3 N_2) mixture the reaction mechanism by Glarborg et al. [9] can reproduce the trends at initial pressures of 4 and 16 bar although predicting shorter ignition delay times than measured. Again, at a pressure of 1 bar, the prediction cannot keep pace with the increase of ignition delay times at lower temperatures.

Next, as it has been presented already for ethene / nitrous oxide mixtures [6], laminar flame speeds will be measured for ethane / nitrous oxide mixtures to provide a complementary validation data set that is especially sensitive to high temperature nitrogen chemistry. This is very important for a good predictive capabilty of combustion CFD-codes modeling rocket combustors for green propellants.

Acknowledgements

The authors thank Juan Ramon Diaz Moralejo, Abhishek Verma, Helena Eulalia Cano Fornos, Robert Djuric and Myles Zabel for their support.

References

[1] Tiliakos, N.; Tyll, J. S.; Herdy, R.; Sharp, D.; Moser, M.; Smith, N., „Development and Testing of a Nitrous Oxide / Propane Rocket Engine," in *AIAA 2001-3258*, 2001.

[2] Keller, J., „AEROSPACE DEFENSE MEDIA GROUP, Intelligent Aerospace," 01 06 2012. [Online]. Available: https://www.intelligent-aerospace.com/articles/2012/06/darpa_works_withfiveaerospacecompaniestodevelopinexpensivelaunch.html. [Zugriff am 18.03.2019].

[3] Werling, L.; Jooß, Y.; Wenzel, M.; Ciezki, H.; Schlechtriem, S., „A premixed Green Propellant consisting of N_2O and C_2H_4: Experimental analysis of quenching diameters to design flashback arresters," in *International Symposium on Special Topics in Chemical Propulsion & Energetic Materials (11-ISICP)*, Stuttgart, 2018.

[4] Werling, L.; Hochheimer, B.; Baral, B.; Ciezki, H.; Schlechtriem, S., "Experimental and Numerical Analysis of the Heat Flux Occurring in a Nitrous Oxide / Ethene Green Propellant Combustion Demonstrator," in *AIAA 2015-4061*, 2015.

[5] Werling, L.; Lauck, F.; Freudenmann, D.; Röcke, N.; Ciezki, H.; Schlechtriem, S., „Experimental Investigation of the Flame Propagation and Flashback Behavior of a Green Propellant Consisting of N_2O and C_2H_4," *J. Energy and Power Engineering,* Bd. 11, pp. 735-752, 2017.

[6] Naumann, C.;, Kick, Th.;, Methling, T.;, Braun-Unkhoff, M.;, Riedel, U., „Ethene / Dinitrogen Oxide - A Green Propellant to substitute Hydrazine: Investigation on its Ignition Delay Time and Laminar Flame Speed," in *Proceedings of the 26th International Colloquium on the Dynamics of Explosions and Reactive Systems (ICDERS)*, Boston, 2017; (available at https://elib.dlr.de).

[7] Naumann, C.; Kick, Th.; Methling, T.; Braun-Unkhoff, M.; Riedel, U., „Ethene / Nitrous Oxide Mixtures as a Green Propellant to substitute Hydrazine: Reaction Mechanisms Validation," in *11th International Symposium on Special Topics in Chemical Propulsion & Energetic Materials (11-ISICP)*, Stuttgart, 2018.

[8] Kick, Th.; Starcke, J.H.; Naumann, C., „Green Propellant Substituting Hydrazine: Investigation of Ignition Delay Time and Laminar Flame Speed of Ethene / Dinitrogen Oxide Mixtures," in *Proceedings of the 8th European Combustion Meeting (ECM)*, Dubrovnik, 2017; (available at https://elib.dlr.de).

[9] Glarborg, P.; Miller, J.A.; Ruscic, B.; Klippenstein, S.J., "Modeling nitrogen chemistry in combustion," *Progress in Energy and Combustion Science,* vol. 67, pp. 31-68, 2018.

[10] Kathrotia, T.; Riedel, U.; Seipel, A.; Moshammer, K.; Brockhinke, A.;, „Experimental and numerical study of chemiluminescent species in low-pressure flames," *Applied Physics B,* Bd. 3, pp. 571 – 584, 2012.

[11] Z. Hong, G. Pang, S. Vasu, D. Davidson und R. Hanson, „The use of driver inserts to reduce non-ideal pressure variations behind reflected shock waves," *Shock Waves,* Bd. 19, pp. 113-123, 2009.

Find this article at DLR's publications database at **https://elib.dlr.de/**